# Traceable size determination of PMMA nanoparticles based on Small Angle X-ray Scattering (SAXS)

Journal of Physics: Conference Series **247** (2010) 012027 doi:10.1088/1742-6596/247/1/012027

# Traceable size determination of PMMA nanoparticles based on Small Angle X-ray Scattering (SAXS)

**G Gleber**[1], **L Cibik**[1], **S Haas**[2], **A Hoell**[2], **P Müller**[1] **and M Krumrey**[1]

[1]Physikalisch-Technische Bundesanstalt (PTB), Abbestrasse 2-12, 10587 Berlin, Germany
[2]Helmholtz-Zentrum-Berlin für Materialien und Energie (HZB), Albert-Einstein-Strasse 15, 12489 Berlin, Germany

E-mail: gudrun.gleber@ptb.de

**Abstract**. The size and size distribution of PMMA nanoparticles has been investigated with SAXS (small angle X-ray scattering) using monochromatized synchrotron radiation. The uncertainty has contributions from the wavelength or photon energy of the radiation, the scattering angle and the fit procedure for the obtained scattering curves. The wavelength can be traced back to the lattice constant of silicon, and the scattering angle is traceable via geometric measurements of the detector pixel size and the distance between the sample and the detector. SAXS measurements and data evaluations have been performed at different distances and photon energies for two PMMA nanoparticle suspensions with low polydispersity and nominal diameters of 108 nm and 192 nm, respectively, as well as for a mixture of both. The relative variation of the diameters obtained for different experimental conditions was below ± 0.3 %. The determined number-weighted mean diameters of (109.0 ± 0.7) nm and (188.0 ± 1.3) nm, respectively, are close to the nominal values.

## 1. Introduction

Nanoparticles are of a growing importance for many areas of modern life, such as medicine (e.g. drug delivery [1]), transport technology (e.g. fuel additives [2]), industrial production (e.g. catalysis [3]) or cosmetics (e.g. sun blocks [4]). Their properties but also their potential risks are strongly size dependent, thus, size determination is a very critical issue [5].

During the last few years, several nanoparticle reference materials have been developed [6], and many different methods have become available to measure nanoparticle size and size distribution [7]. However, the results are not always consistent, even if small uncertainties are indicated for the individual methods. An example is the reference material 8011 of the National Institute of Standards & Technology (NIST) [8] which consists of colloidal gold spheres of a nominal diameter of 10 nm. The average diameter indicated in the report of investigation varies between (8.5 ± 0.1) nm measured by Atomic Force Microscopy (AFM) and (13.5 ± 0.1) nm obtained by Dynamic Light Scattering (DLS).

The aim of the international Joint Research Project "Traceable characterization of nanoparticles" [9] in the framework of the European Metrology Research Programme (EMRP) is to provide new traceable standards and procedures to determine the size, shape and size distribution of nanoparticles with high accuracy. Here traceable refers to the SI units. Several national metrology

 

institutes are participating in this project: the National Physical Laboratory (NPL, UK), the Mittatekniikan keskus (MIKES, Finland), the Bundesamt für Metrologie (METAS, Switzerland), the Istituto Nazionale di Ricerca Metrologica (INRIM, Italy), the Centro Espanol de Metrologia (CEM, Spain), the Institutul National de Metrologie (INM, Romania), the Czech Metrology Institute (CMI), and the Physikalisch-Technische Bundesanstalt (PTB, Germany).

Several different methods will be compared, such as Dynamic Light Scattering (DLS), Small Angle X-ray Scattering (SAXS), Scanning Force Microscopy (SFM) and Scanning Electron Microscopy (SEM). SEM will also be applied in transmission geometry [10]. The scattering methods DLS and SAXS are well suited for measuring the size and size distribution of a particle ensemble, because they deliver information about the huge number of particles from a single measurement. However, DLS is an indirect method relying on the Brownian motion of particles in a suspension of known temperature and viscosity. SAXS in contrast is based on straight-forward X-ray scattering [11]. For almost monodispersed particles, the scattering pattern shows concentric rings with a diameter directly related to the mean diameter of the particles. The achievable uncertainty should be rather low, which was not the case for the SAXS results of small gold nanoparticles (nominal diameter 10 nm) in the NIST report of investigation [8]. Recently, the diameters of these gold nanoparticles have been determined by SAXS with significantly lower uncertainties [12].

## 2. SAXS measurements

The SAXS measurements presented here for traceable size determination were performed on poly-methyl-methacrylate (PMMA) particles obtained from the company microparticles GmbH, Berlin, Germany. The nominal diameter of the investigated particles in aqueous suspension was 108 nm and 192 nm, respectively. The suspension (nominal concentration 10 % w/v) was injected into glass capillaries with a 1 mm diameter and a wall thickness of 10 µm. In addition, a mixture (approximately equal particle masses) of both particle sizes was prepared and other capillaries were filled with distilled water for background subtraction. After filling up to a few cm, the capillaries were hermetically sealed by welding.

The measurements were conducted with synchrotron radiation at the four-crystal monochromator beamline in the laboratory of PTB at the electron storage ring BESSY II [13]. At this beamline, any photon energy in the range from 1.75 keV to 10 keV is available by using either InSb (111) or Si (111) crystals in the monochromator. Different motor-controlled sets of slits in this 37 m long UHV beamline were used to produce a well-defined monochromatic photon beam with an approximately 0.5 mm diameter and a spectral resolving power of about $10^4$.

Up to 15 capillaries can be loaded via a load-lock in the UHV reflectometer allowing for the rotation and the translation of the samples in all degrees of freedom [14]. The last guard slit is already in the reflectometer, only a few cm in front of the sample. Directly behind the reflectometer, the SAXS setup of the HZB is installed, mainly consisting of an adjustable and tiltable, 3 m long support structure, an MAR CCD-based detector of 165 mm diameter and long edge-welded bellows with a 250 mm inner diameter to vary the distance between he sample and the detector continuously without breaking the vacuum [15]. The direct beam is blocked by a beamstop with an area of 1 cm². It is located directly in front of the detector and can be translated horizontally and vertically by ± 6 mm. The SAXS setup and the reflectometer are placed on motorized platforms for alignment with respect to the incoming beam. Both instruments are shown in figure 1. The suspension-filled capillaries in the reflectometer sample holder are enlarged in the inset. The entire beamline, including the monochromator, mirrors, slit systems, the reflectometer and the SAXS setup, is completely computer-controlled. The incident photon flux and the sample transmittance are measured by means of calibrated semiconductor photodiodes.

For the traceable size determination of nanoparticles, the position of the maxima and minima on the momentum transfer axis has to be known precisely, while a calibration of the scattered intensity is not required. For the momentum transfer, the scattering angle and the wavelength have to be calibrated. For the wavelength, back-reflection of radiation from silicon crystals can be used [13], relating the

wavelength (or photon energy) scale of the monochromator to the precisely known lattice constant of silicon [16]. The resulting relative uncertainty of the wavelength is about $10^{-4}$. For the scattering angle, the distance between the detector and the sample as well as the pixel size of the detector has to be known. Both values can be determined by using features of the HZB SAXS setup. The pixel size is obtained by translations of the detector perpendicular to the beam direction. Pictures of the direct but strongly attenuated beam are taken at different displacements which can be measured precisely using a Heidenhain encoder. A pixel size of $(78.94 \pm 0.04)$ µm was obtained, close to the manufacturer's specification. The distance can not be measured directly, but strongly-structured scattering patterns can be recorded at different distances and the change of the distance can be measured with the built-in 3 m long Heidenhain encoder with an uncertainty of 20 µm. By triangulating to the source point, the sample-detector distance can be determined with an uncertainty of below 1 cm. The total relative uncertainty for the distance and the pixel size is about 0.5 %. Further improvements have been initiated to reduce these uncertainties.

The measurements were performed at two different distances (2.03 m and 4.34 m) and at photon energies of 6 keV, 8 keV and 10 keV, respectively. Long exposure times of up to 1 h were used to obtain high-quality data sets.

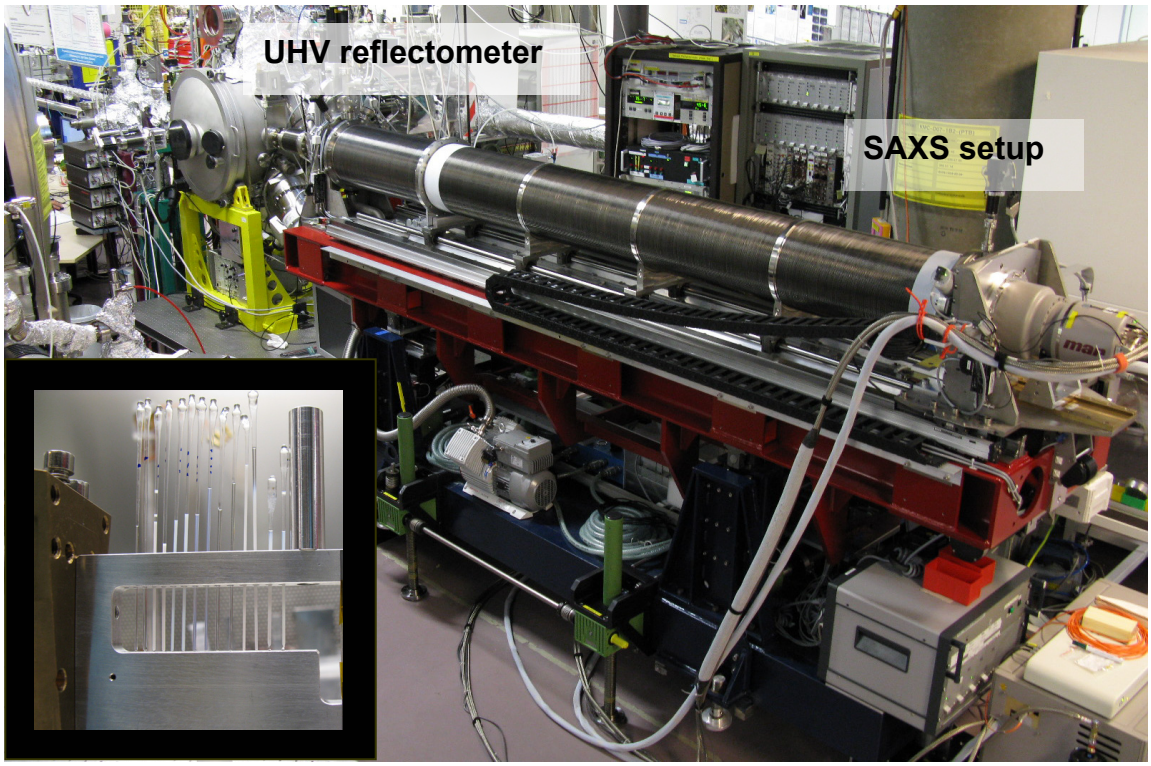


**Figure 1.** UHV reflectometer for sample positioning and SAXS setup including long edge-welded bellows and a CCD-based large-area detector. The inset shows sealed glass capillaries in the sample holder of the UHV reflectometer.

## 3. Results

Scattering patterns recorded for 8 keV radiation with the CCD-based detector at a distance of 2.05 m from the samples are presented in figure 2. The concentric rings are easily seen. While the rings are equally spaced for samples containing only one particle size, the obtained structure for the mixture is more complex. Similar pictures were obtained for all investigated photon energies and both distances. From each picture, a dark image was first subtracted to remove the readout noise of the camera. To subtract a background image of a capillary filled with distilled water, the images were normalized with

the measurement time, the incident beam intensity, and the transmittance of the sample. The shadow of the beamstop was masked, traces of cosmic rays removed, the center was determined and the flat image was projected to a spherical surface. Then the data were circularly integrated to obtain the scattered intensity as a function of the momentum transfer. The scattered intensity curves were fitted with the program SASfit [17] as the sum of background and particle contributions. For a Gaussian distribution of spherical particles with constant electron density, their mean diameter, the width of the distribution and the product of the particle number and the density contrast are the only free parameters. In the evaluated momentum transfer range, contributions from particle interactions can be neglected for the investigated particles sizes and concentrations. The measured and fitted scattering intensities are also shown in figure 2.

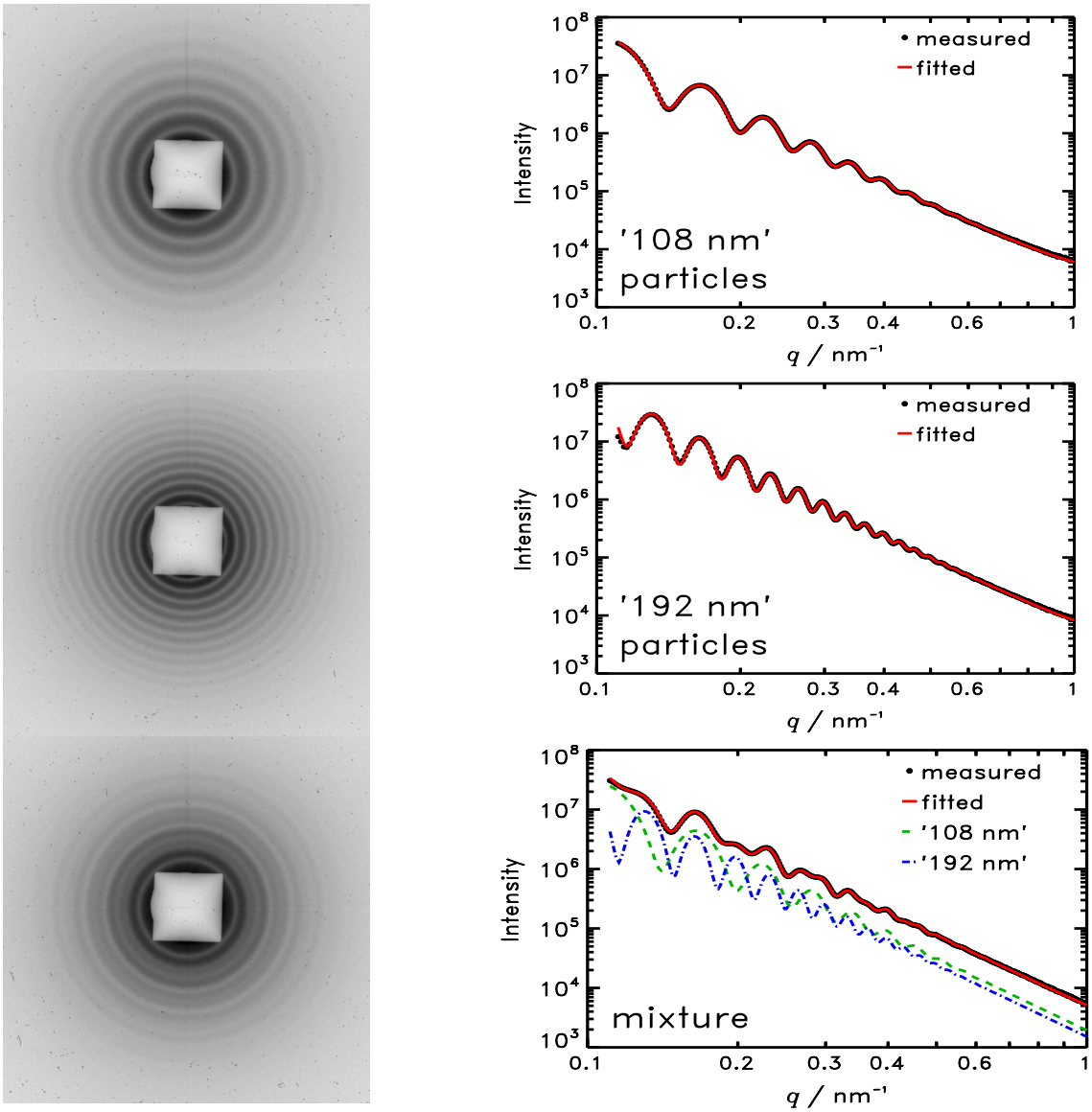


**Figure 2.** Left: Scattering patterns recorded at 8 keV with the CCD-based detector at a distance of 2.04 m from the sample position, for samples containing particles with different nominal diameters: top: '108 nm', center: '192 nm', bottom: mixture of both diameters.
Right: Corresponding circularly integrated scattered intensity and fit results from SASfit assuming a Gaussian distribution.

All results obtained for the number-weighted mean diameter as well as for the width of the Gaussian distribution curve are summarized in table 1. As the distributions are relatively narrow, there is little difference between Gaussian distribution and LogNorm or Schulz-Zimm distribution as also shown recently for gold nanoparticles [12]. The obtained values for the mean diameter exhibit very little variation below ± 0.3 % for different distances and even different photon energies. The results for the mixture and the individual measurements of both particle types are also in agreement within about 0.1 %.

**Table 1.** Number-weighted mean diameter and FWHM of the Gaussian distribution curve obtained at different photon energies and different distances between sample and detector for PMMA particles of two sizes as well as for a mixture of both.

| Nominal diameter (nm) | Photon energy (keV) | Distance (m) | '108 nm' particles | | '192 nm' particles | |
|---|---|---|---|---|---|---|
| | | | Mean diameter (nm) | FWHM (nm) | Mean diameter (nm) | FWHM (nm) |
| **108** | 6 | 2.04 | 108.9 | 12.1 | - | - |
| **108** | 6 | 4.33 | 108.9 | 13.4 | - | - |
| **108** | 8 | 2.05 | 109.2 | 11.2 | - | - |
| **108** | 8 | 4.33 | 108.9 | 12.3 | - | - |
| **108** | 10 | 2.03 | 109.1 | 11.1 | - | - |
| **108** | 10 | 4.33 | 108.9 | 12.0 | - | - |
| **Mean values** | | | **108.97** | **12.03** | | |
| **192** | 6 | 2.04 | - | - | 188.1 | 11.1 |
| **192** | 6 | 4.34 | - | - | 188.0 | 10.7 |
| **192** | 8 | 2.04 | - | - | 188.1 | 11.5 |
| **192** | 8 | 4.34 | - | - | 187.8 | 11.1 |
| **192** | 10 | 2.04 | - | - | 188.0 | 11.2 |
| **192** | 10 | 4.34 | - | - | 187.8 | 10.7 |
| **Mean values** | | | | | **187.96** | **11.05** |
| **108 & 192** | 6 | 2.04 | 109.2 | 11.6 | 188.2 | 11.2 |
| **108 & 192** | 6 | 4.34 | 109.0 | 10.4 | 188.2 | 10.4 |
| **108 & 192** | 8 | 2.04 | 109.2 | 10.9 | 188.2 | 11.4 |
| **108 & 192** | 8 | 4.34 | 108.7 | 12.2 | 187.8 | 11.2 |
| **108 & 192** | 10 | 2.04 | 109.0 | 11.9 | 188.2 | 11.0 |
| **108 & 192** | 10 | 4.34 | 108.8 | 12.0 | 187.9 | 11.2 |
| **Mean values** | | | **108.98** | **11.52** | **188.09** | **11.06** |

The indicated mean diameters are valid for the number-weighted distribution that allows better comparison to microscopic methods. For other weightings, higher values are obtained. However, due to the low polydispersity, the influence of the weighting is small: for the particles with a nominal diameter of 108 nm, the number-weighted mean diameter is 109.0 nm, volume weighting results in a diameter of 109.7 nm, and intensity weighting leads to 110.3 nm, thus, the total variation is about ± 0.6 %. For the larger particles with a nominal diameter of 192 nm, the effect is even smaller with a variation of only ± 0.2 %. The total relative uncertainty for the size determination for the investigated PMMA particles of currently 0.7 % is dominated by the uncertainties of the sample detector distance and contributions from the fitting procedure.

## 4. Conclusion

The mean diameter of PMMA particles in liquid suspension has been determined using SAXS with a small relative uncertainty of about 0.7 %. To further reduce the uncertainty, the measurement capabilities for the geometrical quantities will be improved. Measurements on nanoparticles in the diameter range between 10 nm and 100 nm have been started to extend the accessible diameter range. In the framework of the JRP project "Nanoparticles", the results will be compared to data obtained by DLS and microscopic methods like SEM and AFM.

## References

[1] Olivier J 2005 Drug transport to brain with targeted nanoparticles *NeuroRx.* **2** 118–19
[2] Jung H, Kittelson D B and Zachariah M R 2005 The influence of a cerium additive on ultrafine diesel particle emissions and kinetics of oxidation *Combustion and Flame* **142** 276–88
[3] Jøgensen B, Kristensen S B, Kunov-Kruse A J, Fehrmann R, Christensen C H and Riisager A 2009 Gas-phase oxidation of aqueous ethanol by nanoparticle vanadia/anatase catalysts *Topics in Catalysis* **52** 253–7
[4] Wissing S A and Müller R H 2003 Cosmetic applications for solid lipid nanoparticles (SLN) *Int. J. Pharm.***254** 65–8
[5] Seaton A, Tran L, Aitken R and Donaldson K 2009 Nanoparticles, human health hazard and regulation *Journal of The Royal Society Interface* **7** 119–29
[6] www.nano-refmat.bam.de
[7] Borchert H, Shevehenko EV, Robert A, Mekis I, Kornowski A, Grubel G and Weller H 2005 Determination of nanocrystal sizes: A comparison of TEM, SAXS, and XRD studies of highly monodisperse CoPt3 particles *Langmuir* **21** 1931-6
[8] National Institute of Standards and Technology (NIST) 2007 Report of investigation, Reference Material 8011, Gaithersburg, USA
[9] Euramet, T3.J1.1, http://www.euramet.org/index.php?id=1011
[10] Buhr E, Senftleben N, Klein T, Bergmann D, Gnieser D, Frase C G and Bosse H 2009 Characterization of nanoparticles by scanning electron microscopy in transmission mode *Measurement Science and Technology* **20** 084025
[11] Glatter O and Kratky O 1982 *Small-angle X-ray Scattering* (London: Academic Press)
[12] Bienert R, Emmerling F and Thünemann A F 2009 The size distribution of 'gold standard' nanoparticles *Anal. Bioanal. Chem.* **395** 1651–60
[13] Krumrey M and Ulm G 2001 High-accuracy detector calibration at the ptb four-crystal monochromator beamline *Nucl. Instr. and Meth.* **467–468** 1175–8
[14] Fuchs D, Krumrey M, Müller P, Scholze F and Ulm G 1995 High precision soft X-ray reflectometer *Rev. Sci. Instr.* **66**, 2248-50
[15] Hoell A, Zizak I, Bieder H and Mokrani L 2007 German patent 10 2006 029 449
[16] Massa E, Mana G and Kuetgens U 2009 Comparison of the INRIM and PTB lattice-spacing standards *Metrologia* **46** 249–53
[17] Kohlbrecher J 2009 SASfit. PSI, Laboratory for Neutron Scattering ETHZ & PSI CH-5232 Villigen PSI, Switzerland, 0.92.2 edition http://kur.web.psi.ch/sansl/SANSS0ft/sasfit.html